Available online at www.sciencedirect.com
SCIENCE DIRECT®
International Journal of Thermal Sciences 43 (2004) 3–11
International Journal of Thermal Sciences
www.elsevier.com/locate/ijts

Time-dependent buoyant convection in an enclosure with discrete heat sources

Jun Ho Bae, Jae Min Hyun *

Department of Mechanical Engineering, Korea Advanced Institute of Science & Technology, 373-1 Kusong-dong, Yusong-gu, Taejon 305-701, South Korea

Received 9 January 2003; accepted 27 March 2003

Abstract

A numerical study is performed for the time-dependent laminar natural convection air cooling in a vertical rectangular enclosure with three discrete flush-mounted heaters. The lowest-elevation heater changes the thermal condition between the 'on' and 'off' modes. In Case 1 (Case 2), the lowest-elevation heater is abruptly switched on (off) from the 'off' ('on') state. In Case 3, the 'on' and 'off' modes are repeated periodically. Numerical simulations were conducted for a range of non-dimensional period and for the Rayleigh number based on the cavity width between 10^5 and 10^7 with given heater size and locations. The results show the influence of the time-dependent thermal condition of the lowest-elevation heater on the temperatures of the other heaters. At low Rayleigh number, the cycle-averaged temperatures of all heaters are little affected by the periodic change. At high Rayleigh number, the temperatures of the heaters reach peak values when the non-dimensional period of the change in thermal condition takes intermediate values. The evolutions of global flow and temperature fields are exemplified to provide physical interpretations. The study emphasizes that the transient-stage temperatures at the heaters can exceed the corresponding steady-state values. This is relevant to practical design of electronic devices.

1. Introduction

Effective cooling of electronic devices in an enclosed space warrants an in-depth scrutiny. One buoyant-convective flow layout is illustrated in Fig. 1. The electronic components are modeled as discrete heat sources on one vertical sidewall, and the opposite vertical sidewall is maintained at a lower temperature [1–4]. Based on numerical and/or experimental endeavors, several correlations have been presented in the literature for the Nusselt number and the temperatures of the heaters. Among others, it was learned that a discretely-heated vertical wall leads to a higher heat transfer coefficient than a cavity with a fully-heated vertical wall [2].

In the analysis of buoyant convection due to multiple heat sources, the important flow ingredient is the interactions in the thermal wake of a bottom heater and the heaters located above. The optimum design of electronic packages which

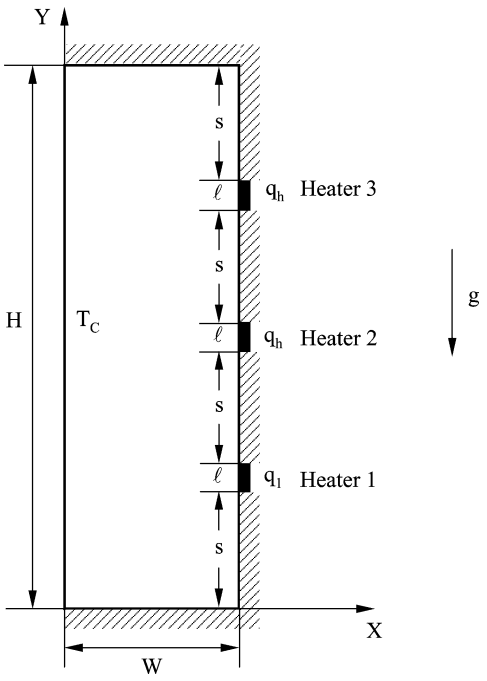

Fig. 1. Flow layout and the coordinates.

* Corresponding author.
E-mail address: jmhyun@kaist.ac.kr (J.M. Hyun).

1290-0729/$ – see front matter
doi:10.1016/S1290-0729(03)00102-9

Nomenclature

g	gravitational acceleration
H	height of the cavity
k	thermal conductivity
l	length of a heater
q_{h}	heat flux of a heater
p, P	dimensional and non-dimensional pressure
Pr	Prandtl number, $Pr = \nu/\alpha$
Ra	Rayleigh number, $Ra = g\beta q_h W^4/k\nu\alpha$
s	dimensional spacing between discrete heaters
t	dimensional time
T	dimensional temperature
U, V	non-dimensional velocity components in the X and Y directions
W	width of enclosure
x, y	dimensional horizontal and vertical coordinates
z, Z	dimensional and non-dimensional period, $Z = z\alpha/W^2$

Greek symbols

α	thermal diffusivity
β	isobaric coefficient of volumetric thermal expansion
ρ	density
τ	non-dimensional time
ν	kinematic viscosity
θ	non-dimensional temperature
θ_m	non-dimensional surface-averaged temperature of a heater
θ_{on}, θ_{off}	the steady-state temperature of Case 1, Case 2
$\overline{\theta}$	cycle-averaged temperature of a heater, Eq. (7)
Θ	temperature amplification factor for a given heater, Eq. (8)
Ψ	non-dimensional stream function

would improve the overall cooling of a multi-component system was explored [5,6]. It was also revealed that the two-dimensional model predicts reasonably well the general trends of realistic systems [7].

It is noted that the majority of preceding investigations dealt with the steady-state characteristics. However, knowledge on the time-dependent responses of the thermal systems during the switching-on and switching-off and other time-variant changes in thermal environment is essential in the setup and operation of modern high-tech electronic devices. Studies on such transient characteristics in an enclosure with multiple heat sources are scarce [8–10]. Of particular interest to practical applications is the requirement that the maximum temperature of the system component be below a certain threshold value. The present study aims to delineate the transient flow characteristics in a rectangular enclosure with multiple electronic components. The time-dependent flows are induced by the energizing (on) or the de-energizing (off) modes of the heaters. As documented in the prior accounts, the influence of the lower-elevation heater on the higher-elevation heaters is more pronounced due to the interactions of the thermal wake of a lower-elevation heater. In the present paper, for definiteness, the thermal condition at the lowest-elevation heater alternates between the 'on' and 'off' modes while the rest of the heaters maintain the 'on' mode. Detailed numerical computations are conducted, and physical interpretations of the results will be provided.

The purpose is to demonstrate that the transient temperatures at the heaters may become higher than their steady-state values. Also, the increases in the maximal temperatures at the heaters are shown to be affected appreciably by the change in the period of time-varying thermal condition. These issues will be of concern to the design and operation of the thermal system involving electronic devices.

2. Model

The schematic of the two-dimensional physical system and the coordinates are sketched in Fig. 1. The rectangular cavity (width W, height H) is filled with an incompressible Boussinesq fluid, which satisfies $\rho = \rho_{\mathrm{r}}[1 - \beta(T - T_{\mathrm{r}})]$, β being the coefficient of thermometric expansion, and subscript r denoting the reference state. All other physical properties are taken to be constant. The temperature at the cold left vertical sidewall is constant T_{C}, and the top and bottom horizontal walls are insulated. As a paradigmatic geometry [1], three discrete heaters of length l each are flushed-mounted at the right vertical wall with equal spacing s. The heat flux generated by each heater is q_{h}.

The governing time-dependent Navier–Stokes equations, in non-dimensional form, are [10]:

Continuity

$$\frac{\partial U}{\partial X} + \frac{\partial V}{\partial Y} = 0 \tag{1}$$

Momentum

$$\frac{\partial U}{\partial \tau} + \frac{\partial}{\partial X}\left(U^2\right) + \frac{\partial}{\partial Y}(VU) = -\frac{\partial P}{\partial X} + Pr \cdot \nabla^2 U \tag{2}$$

$$\frac{\partial V}{\partial \tau} + \frac{\partial}{\partial X}(UV) + \frac{\partial}{\partial Y}\left(V^2\right) = -\frac{\partial P}{\partial Y} + (Pr \cdot Ra)\theta + Pr \cdot \nabla^2 V \tag{3}$$

Energy

$$\frac{\partial \theta}{\partial \tau} + \frac{\partial}{\partial X}(U\theta) + \frac{\partial}{\partial Y}(V\theta) = \nabla^2 \theta \tag{4}$$

where

$$\nabla^2 = \frac{\partial^2}{\partial X^2} + \frac{\partial^2}{\partial Y^2} \tag{5}$$

In the above, non-dimensionalization has been implemented by using

$$\tau = t\alpha/W^2, \quad (X,Y) = (x,y)/W, \quad (U,V) = (u,v)W/\alpha$$
$$\theta = (T - T_c)/(q_h W/k), \quad P = (p + \rho g y)W^2/\rho\alpha^2$$
$$Ra = g\beta q_h W^4/k\nu\alpha, \quad Pr = \nu/\alpha$$

In the present formulation, the cavity width W was chosen as the characteristic length. This is in accord with the non-dimensionalization scheme of Ref. [1], which considered a similar geometrical arrangement.

The boundary conditions at the enclosure walls are:

$$\text{at } Y = 0.0, H/W \quad U = V = \frac{\partial\theta}{\partial Y} = 0 \tag{6a}$$
$$\text{at } X = 0.0 \quad U = V = 0, \theta = 0 \tag{6b}$$
$$\text{at } X = 1.0 \quad U = V = 0 \tag{6c}$$
$$\text{at } X = 1.0 \quad \frac{\partial\theta}{\partial X} = 1 \quad \text{(at heater 2, heater 3)}$$
$$\frac{\partial\theta}{\partial X} = 0 \quad \text{(elsewhere)} \tag{6d}$$

Three types of time-dependent heat-flux conditions at the lowest-elevation heater 1 are considered (see Fig. 2). In Case 1, heater 1 is suddenly switched on at $\tau = 0$ from the 'off' state. Case 2 depicts the opposite situation of switching off heater 1 at $\tau = 0$ from the 'on' state. In Case 3, the 'on' and 'off' modes of heater 1 are repeated periodically in a square-wave form with non-dimensional period Z [$\equiv z\alpha/W^2$]. The thermal boundary condition at heater 1 can be expressed as follows:

$$\text{Case 1:} \quad \frac{\partial\theta}{\partial X} = 0(\tau < 0), \quad \frac{\partial\theta}{\partial X} = 1(\tau \geqslant 0)$$
$$\text{Case 2:} \quad \frac{\partial\theta}{\partial X} = 1(\tau < 0), \quad \frac{\partial\theta}{\partial X} = 0(\tau \geqslant 0)$$
$$\text{Case 3:} \quad \frac{\partial\theta}{\partial X} = 1\left(nZ \leqslant \tau < \frac{Z}{2} + nZ\right)$$
$$\frac{\partial\theta}{\partial X} = 0\left(\frac{Z}{2} + nZ \leqslant \tau < Z + nZ\right)$$
$$n = 1, 2, \ldots$$

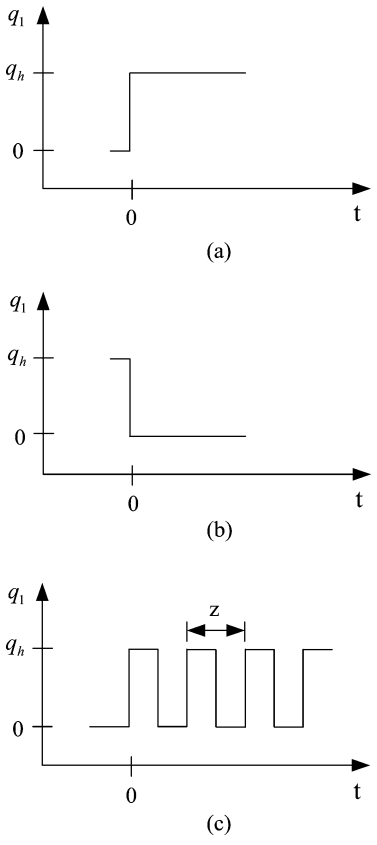

Fig. 2. Types of time-dependent thermal boundary conditions at heater 1. (a) Case 1; (b) Case 2; (c) Case 3.

The above system of equations was solved numerically by employing a finite-volume procedure based on the SIMPLER algorithm [11]. The central differencing was adopted for the diffusion terms, and a modified version of the QUICK scheme was utilized for the nonlinear convective terms [12]. Convergence at a given time step was declared when the maximum relative change between two consecutive iteration levels fell below 10^{-4} for U, V, θ. A parallel check was made to ensure that the energy balance between the heaters and the cold wall was met within 0.2%.

Numerical results were checked for grid- and time-step convergence. Based on these tests, a uniform grid of 151 in the y direction and a non-uniform grid of 61 in the x direction were selected for the present calculations. The time step of $\Delta\tau = 10^{-5}$ was chosen. Under-relaxation was not required to obtain convergence. These exercises established the accuracy and robustness of the present numerical methodologies. No claims are made here as to the innovativeness of the numerical techniques. The calculations were performed in a routine manner. The emphasis is placed on extracting physically meaningful interpretations out of the numerical results.

3. Results and discussion

In the present work, the geometrical particulars of the heater arrangements adopted those of [1], i.e., $H/W = 5.0, l/H = 1.0/30.0, s/H = 9.0/50.0, Pr = 0.7$, and the range of $Ra = 10^5 - 10^7$.

The principal features of the steady-state flows are exemplified in Fig. 3. At high Ra, isotherms are clustered in the immediate vicinity of the heaters. These lead to thin boundary-layer flows near the vertical walls. When the lowest-elevation heater 1 is inactive (see Fig. 3(a)), the buoyancy-driven flow is largely confined to the upper part of the cavity above the level of heater 2. In the lower part of the cavity below the level of heater 2, the fluid is substantially isothermal and stagnant. When all three heaters are powered on (see Fig. 3(b)), the global flow throughout the cavity is invigorated. It is noted that, due to the presence of the

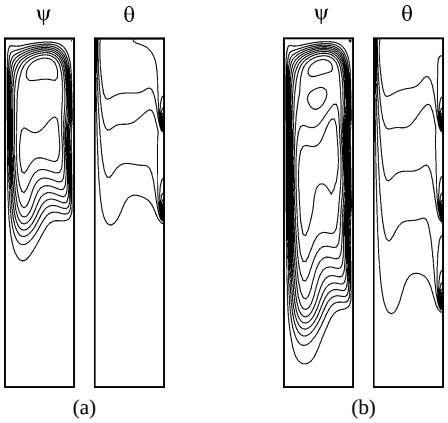

Fig. 3. Stream functions (ψ) and i sotherms (θ) at the steady state. $Ra = 10^7$. (a) heater 1 in 'off' mode [$\psi_{\max} = 26.54, \theta_{\max} = 0.0588$]; (b) heater 1 in 'on' mode [$\psi_{\max} = 30.70, \theta_{\max} = 0.0624$].

thermal wake of heater 1, buoyant flow in the localized region in the vicinity of heater 2 is intensified.

Now, the time-dependent features are described. Fig. 4 illustrates the temperature histories of the heaters in Case 1 (switch-on of heater 1) and Case 2 (switch-off of heater 1). In the plots, θ_m denotes the averaged value of temperature over the surface of a heater. Note the difference in scales used for the ordinates of the plots. As heater 1 is powered on abruptly (see Figs. 4(a), 4(c), 4(e)), the temperature of heater 1 rises sharply, and it reaches a peak value. However, since buoyant motions are induced near heater 1, the temperature of heater 1 falls afterward due to the incoming cold fluid from below, and then it marches slowly toward the steady-state value. For heater 2 and heater 3, the important dynamic element is the influence of the thermal wake produced by heater 1. The peak values of temperatures of heater 2 and heater 3 are

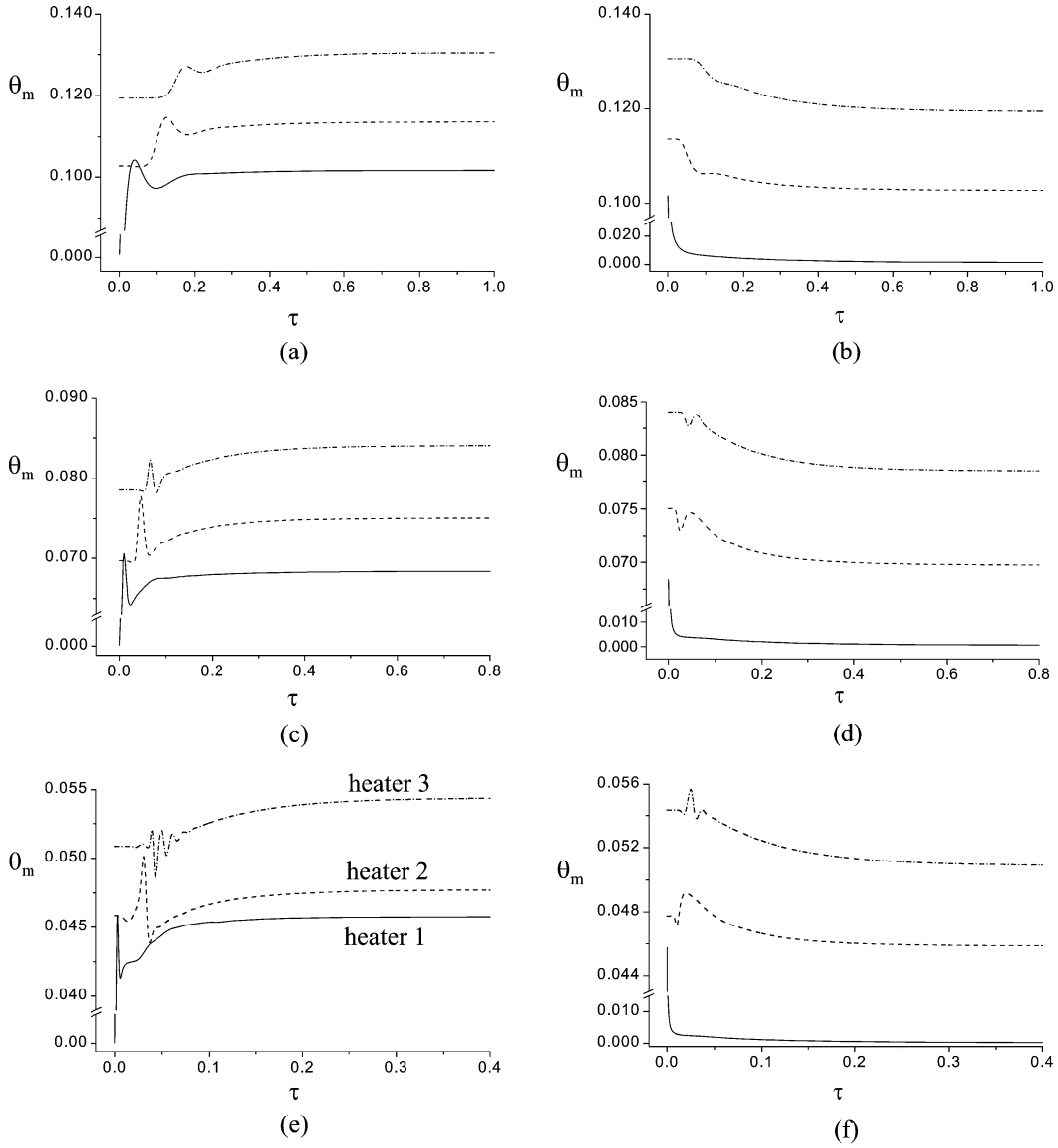

Fig. 4. Temperature histories at the heaters. (a), (b): $Ra = 10^5$; (c), (d): $Ra = 10^6$; (e), (f): $Ra = 10^7$. (a), (c), (e): Case 1; (b), (d), (f): Case 2. (——: heater 1; – – – –: heater 2; —·—: heater 3).

achieved soon after the switch-on. However, after reaching the peak value, the buoyant motion in the thermal wake near heater 2 strengthens, which brings in the relatively cold fluid near heater 1 from below. The response of heater 3 is qualitatively similar to that of heater 2. The temperature peak of heater 3 is smaller than that of heater 2, since the intensity of the thermal wake of heater 1 is reduced as it travels upward further. The above-stated observations are more distinct as *Ra* increases.

On the other hand, when heater 1 is switched off (see Figs. 4(b), 4(d), 4(f)), the temperature of heater 1 decays fast to approach the cold wall temperature. The temperatures of heater 2 and heater 3 decrease slowly toward the steady-state values. It is noticed in Figs. 4(d) and 4(f) that the decay curves of the temperatures of heater 2 and heater 3 show small overshoots at early times. This can also be explained by noting the disappearance of the thermal wake of heater 1 with the switch-off. Near heater 2 and heater 3, buoyant flows weaken quickly, which leads to high temperatures of heater 2 and heater 3. It is recalled that one purpose of the thermal control is to maintain the temperatures of all system components to be below an allowable value. In this respect, the significance of the transient behavior, as well as the steady-state features, is stressed.

The early-time evolutions of flow (ψ) and temperature (θ) fields for $Ra = 10^7$, after the switch-on of heater 1, are exemplified in Fig. 5. At short times, the thermal boundary layer is formed near heater 1 (see Fig. 5(a)). The thermal wake of heater 1 impacts on the region of heater 2, while the intensity of the buoyant flow in this region has not been much affected. Therefore, the temperature of heater 2 records a peak (see Fig. 4(e)) around $\tau = \tau_b$ in Fig. 5. After this stage, the buoyant motion near heater 2 intensifies, which brings forth the entrainment of the relatively cold fluid from the bottom region of the cavity. This causes a decrease in the temperature of heater 2, as indicated in Fig. 4(e). At a later time, the thermal wake of heater 1 reaches the region of heater 3, and a qualitatively similar interpretation can be applied. However, the impact of the thermal wake of heater 1 on the region of heater 3 is less effective since the thermal wake has been weakened by thermal loss to the interior.

The sequential plots for case 2 are exhibited in Fig. 6. With the de-activation of heater 1, the driving buoyancy near heater 1 ceases. At small times, the temperatures of heater 2 and heater 3 rise due to the weakening buoyancy in these localized zones. At later times, the temperature in the interior decreases, and this brings down the temperatures of the heaters accordingly (Figs. 6(c), 6(d)). At large times, the cavity below the elevation of heater 2 is largely stagnant and isothermal.

Next, the numerical results for Case 3 are scrutinized. The time-periodic behavior of temperature and vertical velocity at heater 2 is illustrated in Fig. 7. In the plots, the abscissa shows the passage of time, normalized by the imposed period, τ/Z. The vertical velocity at heater 2 is measured at $(X, Y) = (0.95, 2.5)$. For comparison purposes, the steady-state values of Case 1 and Case 2 are also shown in the figures. When the period Z of the square wave of Case 3 is large, the direct effect of the externally-applied temperature variation at heater 1 is mild. In this case, therefore, the system response is qualitatively similar to that of Case 1 over the first-half of the period and to that of Case 2 over the last-half of the period. Since the period Z is large, these two responses are less overlapping and, therefore, less interacting with each other, as illustrated in the V-plots of Fig. 7(d).

As the period (Z) decreases, the characteristics of Case 1 and Case 2 are mixed and interacting in the results of Case 3. It is recalled that, in Case 1 (abrupt switch-on of heater 1), the buoyancy near heater 2 intensifies after the thermal wake of heater 1 reaches the elevation of heater 2. On the other hand, in Case 2 (abrupt switch-off of heater 1), the buoyancy near heater 2 weakens rapidly. In other words, the build-up of buoyancy near heater 2 progresses comparatively slowly in Case 1, whereas the attenuation of buoyancy near heater 2 takes place relatively rapidly. Consequently, if the switch-on

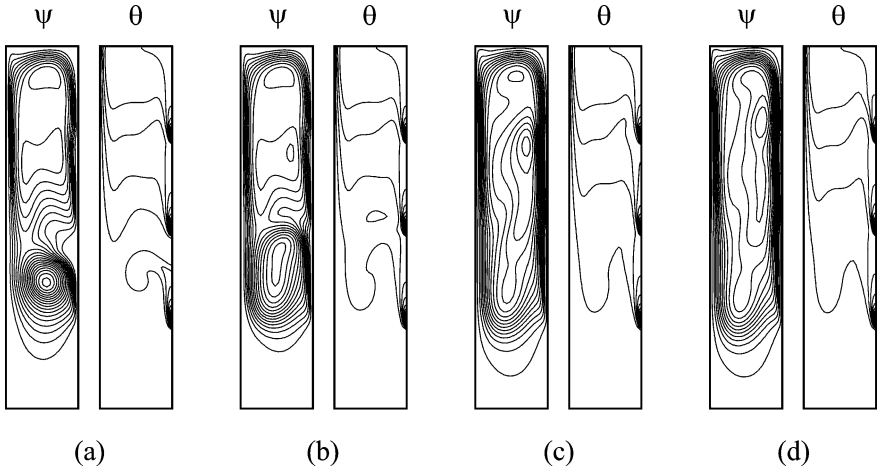

Fig. 5. Sequential plots of flow and temperature fields. Case 1. $Ra = 10^7$. (a) $\tau = \tau_a = 1.5 \times 10^{-2}$; (b) $\tau_b = 3.0 \times 10^{-2}$; (c) $\tau_c = 3.9 \times 10^{-2}$; (d) $\tau_d = 4.3 \times 10^{-2}$. $\Delta\psi = 2.5$, $\Delta\theta = 0.004$.

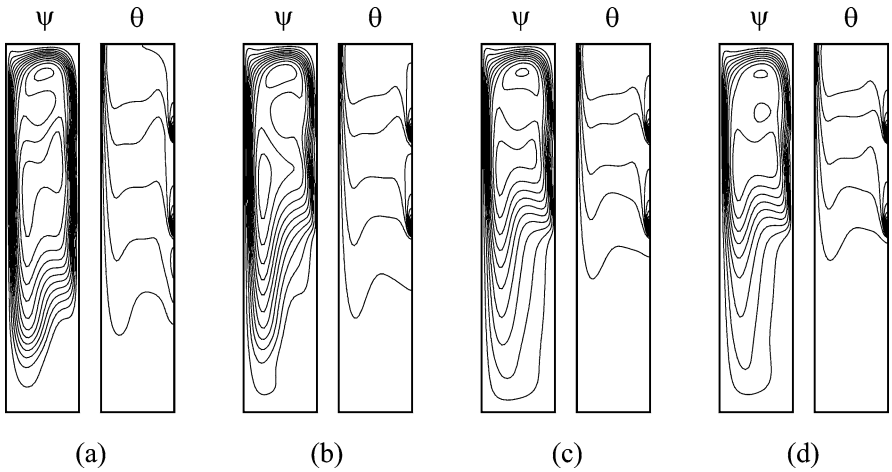

Fig. 6. Same as in Fig. 5, but for Case 2. (a) $\tau = \tau_a = 5.0 \times 10^{-3}$; (b) $\tau_b = 2.0 \times 10^{-2}$; (c) $\tau_c = 5.0 \times 10^{-2}$; (d) $\tau_d = 1.0 \times 10^{-1}$.

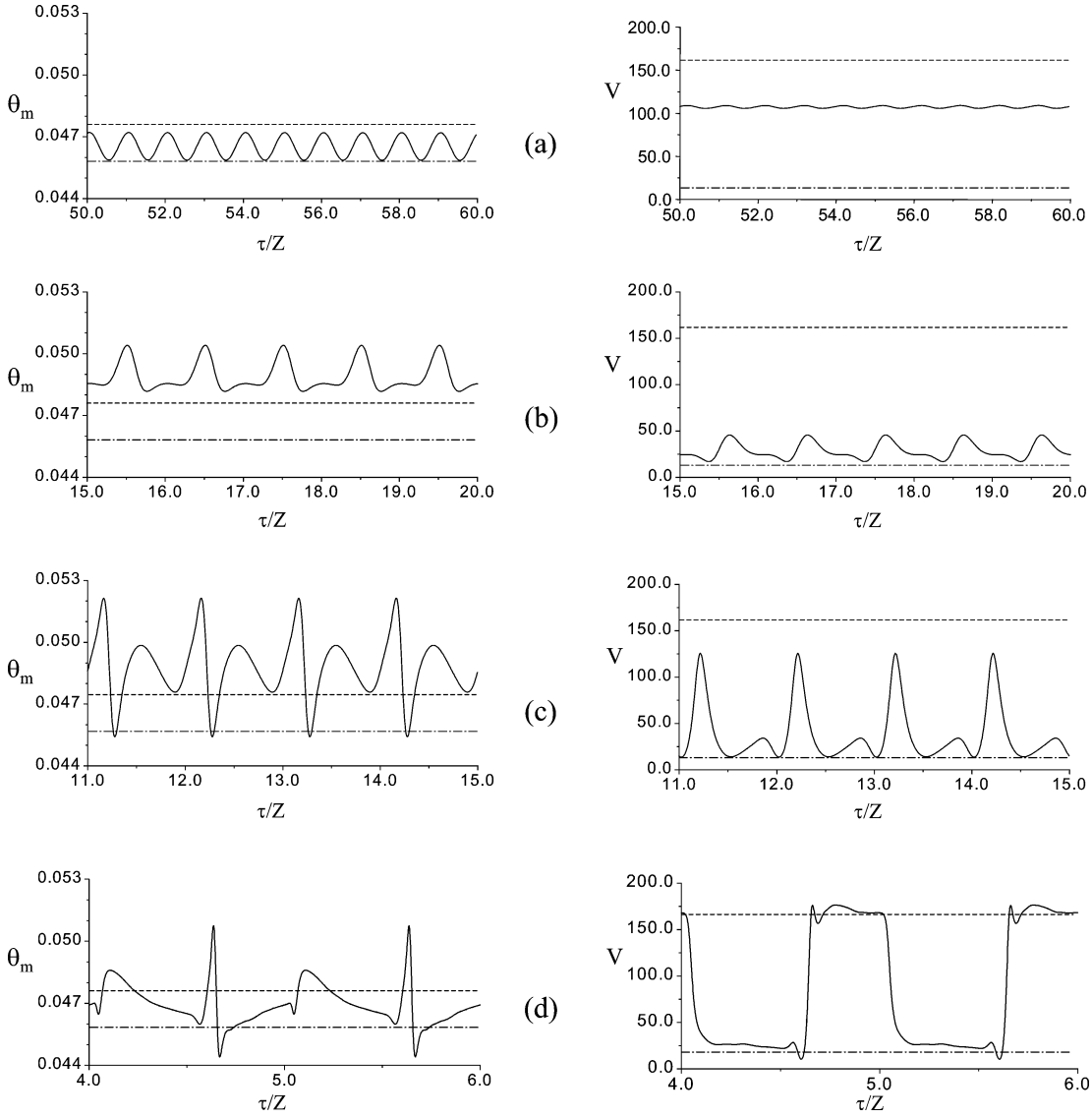

Fig. 7. Histories of temperature (left column) and of vertical velocity (right column) at heater 2. Case 3. $Ra = 10^7$. (a) $Z = 0.006$; (b) $Z = 0.024$; (c) $Z = 0.04$; (d) $Z = 0.2$. (– – – –: steady-state value of Case 1; — · —: steady-state value of Case 2).

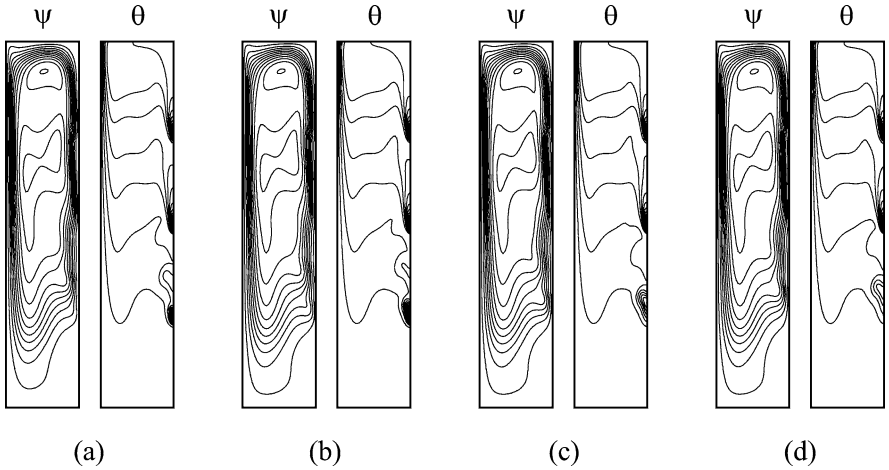

Fig. 8. Sequential plots of stream functions (ψ) and isotherms (θ). $Ra = 10^7$. $Z = 0.006$. (a) $\tau = \tau_a = Z/4$; (b) $\tau_b = 2Z/4$; (c) $\tau_c = 3Z/4$; (d) $\tau_b = 4Z/4$. $\Delta\psi = 2.5$, $\Delta\theta = 0.003$.

and switch-off of heater 1 alternate with the same duration, heater 2 is exposed longer to the condition of relatively weaker buoyancy on the average. These trends become more conspicuous as Z decreases.

As the period Z decreases further, the frequent intermittent thermal forcing is akin to a continuous sinusoidal energizing of heater 1. The response of heater 2 is similar to a sinusoidal variation. Therefore, the interactions occurring due to the effects of the previous cycle and of the present cycle emerge to be a dominant dynamic element. The sequential depictions of flow and thermal fields are given in Fig. 8 for $Z = 0.006$. The thermal wake of heater 1 moves to the region of heater 2 by way of the boundary layer on the heated vertical wall. The bulk of the cavity interior responds to the time-periodic continuous heating from heater 1.

When the period Z takes an intermediate value (see Fig. 9 for $Z = 0.024$), the sequential plots are revealing. As heater 1 is activated at $\tau = \tau_a$ (see Fig. 9(a)), a new circulation cell is formed near heater 1, and the thermal wake of heater 1 grows along the heated vertical wall. It is noted that, due to the effect of the previous cycle, the buoyant flow is less intense in the region below the elevation of heater 2. This implies that the heated fluid from heater 1 takes more time to reach the elevation of heater 2. On the other hand, the effect of the de-activation of heater 1 (see Figs. 9(c) and 9(d)) propagates promptly to the region of heater 2 along the heated vertical wall. As is evident in Fig. 9(d), around $\tau = \tau_d$, the de-activation of heater 1 is felt in the area of heater 2, which weakens the buoyancy in this region. Accordingly, as time elapses from $\tau = \tau_d$ to $\tau = \tau_a$, the increase in buoyancy near heater 2 is not pronounced, as the thermal wake of heater 1 passes by the region of heater 2. On the average, therefore, due to the weakened buoyancy, the temperature of heater 2 for an intermediate value of Z is higher than for larger Z.

For heater 1, 2, 3, the mean temperature of a heater over a cycle, $\bar{\theta}$, is defined as

$$\bar{\theta} = \frac{1}{Z}\int_{\tau_{ss}}^{\tau_{ss}+Z} \theta_m \,\mathrm{d}\tau. \tag{7}$$

It is also useful to gauge the relative increase in temperature at a heater due to the square-wave variation (Case 3) of heating at heater 1. For this purpose, it is advantageous to define the temperature-amplification factor Θ for a given heater as

$$\Theta = \frac{\bar{\theta} - \theta_{off}}{\theta_{on} - \theta_{off}} \tag{8}$$

In the above, $\theta_{on}[\theta_{off}]$ denotes the steady-state temperature of a given heater when heater 1 is in on-mode (Case 1) (off-mode (Case 2)). Therefore, Θ in Eq. (8) indicates the increase in the temperature over the off-mode value, relative to the difference between the values corresponding to the off-mode (Case 2) and on-mode (Case 1).

Fig. 10 illustrates the variations of the temperature amplification factor for a given heater, Θ, versus the period Z. When Z is large, the temperatures of heaters are the steady-state values of Case 1 for nearly a half period and the values of Case 2 for the other half period. Hence, for all the heaters, Θ is close to 0.5, which indicates that the cycle-averaged temperatures of the heaters, $\bar{\theta}$, are the arithmetic mean values of θ_{on} and θ_{off}.

When Z is small, Θ of heater 1 and heater 3 are close to 0.5 for all Ra, while Θ of heater 2 is lower than 0.5 at $Ra = 10^7$. As disclosed in Fig. 8, the frequent thermal forcing from heater 1 forms the momentum boundary layer along the heated vertical wall above heater 1. The average buoyancy force near heater 2 is relatively strong over a period. Hence, Θ of heater 2 is lower than 0.5 at high Ra.

For an intermediate value of Z, heater 2 and heater 3 show different features on the variation of Θ. At $Ra = 10^5$, convection is less influential, and, therefore, Θ of heater 2 and heater 3 are close to the arithmetic mean values of θ_{on} and θ_{off} regardless of Z. As Ra increases, convection prevails, and the dependence of Θ of heater 2 and heater 3 on

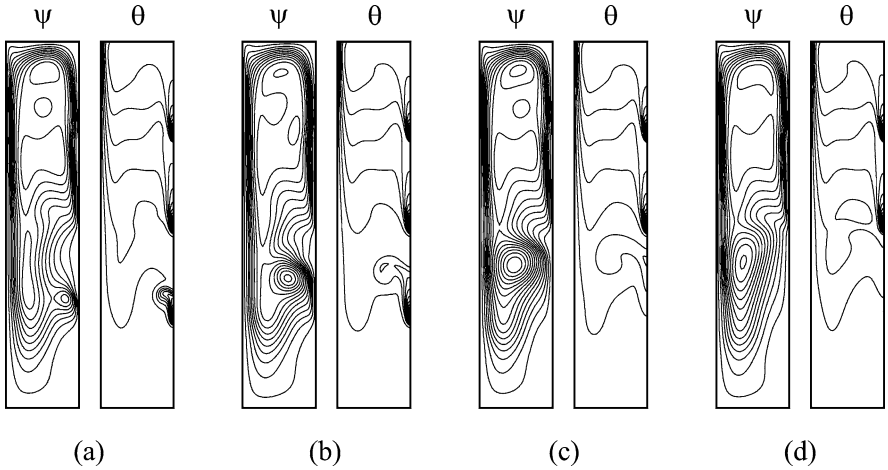

Fig. 9. Same as in Fig. 8, but for $Z = 0.024$.

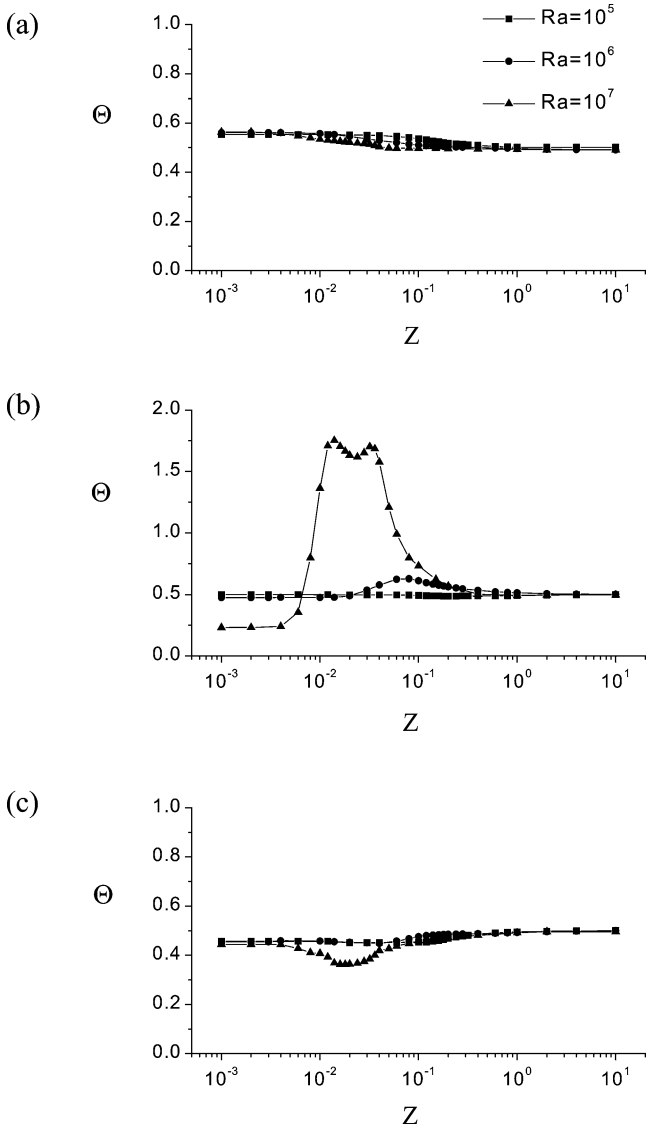

Fig. 10. Variations of the temperature amplification factor for a given heater, Θ, with Z. (a) heater 1; (b) heater 2; (c) heater 3.

Z is pronounced. At $Ra = 10^7$, Θ of heater 2 is maximum at around $Z = 0.024$. It is noted that Θ of heater 2 for this value of Z is higher than 1.0, which reflects that the cycle-averaged temperature, $\bar{\theta}$, is higher than the steady-state temperature of Case 1.

As remarked previously, when Z is intermediate, the thermal effect of de-activation of heater 1 reaches heater 2 before the thermal wake of heater 1 promotes the buoyancy force near heater 2. Thus, the buoyancy force near heater 2 is relatively low. Accordingly, the value of Z, for which heater 2 has the maximum value of Θ, can be deduced from the time needed for the thermal effect of heater 1 to exert influence on heater 2. Fig. 10(b) shows that, as *Ra* decreases, Θ of heater 2 is maximized when Z is slightly larger, which supports the above argument. However, the overall magnitude of the peak is suppressed by the attenuated effect of buoyant convection.

The time-mean flow and temperature fields are described by averaging the time-dependent solutions over a cycle, which are illustrated in Fig. 11. For a large period ($Z = 0.2$), the time-mean solution appears to be similar to the averaged value of the steady-state solutions of Case 1 and Case 2. For a small period ($Z = 0.006$), the momentum boundary layer is distinct in the time-mean solution along the heated vertical wall above heater 1, which strengthens the buoyant convection near heater 2. It is in line with the previous argument that, at high *Ra*, the cycle averaged temperature, $\bar{\theta}$, of heater 2 has a relatively low value when Z is very small. However, for $Z = 0.024$, the time-mean solution reveals that the intensity of buoyancy force is weak along the heated vertical wall below heater 2, especially in the localized region near heater 2. The temperatures in the interior region between heater 1 and heater 2 are higher than those of the case of $Z = 0.2$. These facts are in accord with the previous interpretation for the cycle-averaged temperature of heater 2.

When Z is intermediate, the buoyancy force near heater 3 remains fairly constants over a period (see Fig. 9). As shown in the averaged temperature fields, the thermal wake from heater 1 losses a larger portion of thermal energy into the

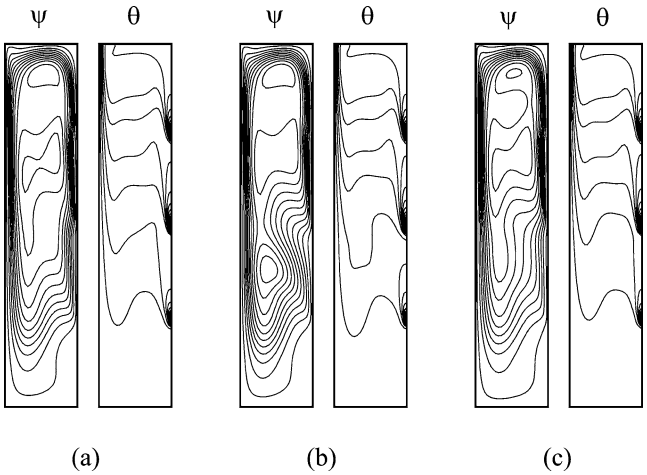

Fig. 11. Time-mean flow and temperature fields. $Ra = 10^7$. (a) $Z = 0.006$ [$\psi_{max} = 27.14$, $\theta_{max} = 0.0609$]; (b) $Z = 0.024$ [$\psi_{max} = 28.02$, $\theta_{max} = 0.0606$]; (c) $Z = 0.2$ [$\psi_{max} = 27.47$, $\theta_{max} = 0.0611$]. $\Delta\psi = 2.5$, $\Delta\theta = 0.003$.

interior region between heater 1 and heater 2. Hence, Θ of heater 3 reaches a minimum at the intermediate period. It is noted that the temperature of heater 3 is the highest among the three heaters. In order to maintain the temperature of the entire system below a threshold value, it is desirable to choose the proper value of the period Z, at which the value of Θ of heater 3 is minimized.

4. Conclusion

In Case 1 and Case 2, the influence of the thermal wake generated by heater 1 and the accompanying buoyant flow near the heaters lead to maximum temperatures of heater 2 and heater 3. These trends are conspicuous at high *Ra*.

In Case 3, the interactions between the effects of Case 1 and Case 2 play a central role on the buoyant flows near heater 2 and heater 3 and on the corresponding temperature changes of heaters. For an intermediate value of the period, the buoyancy force near heater 2 is relatively weak over a period. For a very small value of the period, the momentum boundary layer is formed along the vertical heated wall above the elevation of heater 1 due to a near-continuous thermal forcing at heater 1. The buoyancy force near heater 2 is increased accordingly.

The Θ–Z plots illustrate that, at $Ra = 10^7$, when the period Z is intermediate, Θ of heater 2 reaches a maximum while Θ of heater 3 shows a mild minimum. As *Ra* decreases, the peak values of Θ are less pronounced and they occur at a larger value of Z.

Acknowledgement

Appreciation is extended to the referees for constructive and helpful comments. This work was supported by the National Research Laboratory (NRL) project of South Korea.

References

[1] C.J. Ho, J.Y. Chang, A study of natural convection heat transfer in a vertical rectangular enclosure with two-dimensional discrete heating: effect of aspect ratio, Internat. J. Heat Mass Transfer 37 (1994) 917–925.
[2] M. Keyhani, V. Prasad, R. Cox, An experimental study of natural convection in a vertical cavity with discrete heat sources, J. Heat Transfer 100 (1988) 616–624.
[3] Y. Liu, N.P. Thien, An optimum spacing problem for three chips mounted on a vertical substrate in an enclosure, Numer. Heat Transfer A 37 (2000) 613–630.
[4] G.P. Peterson, A. Ortega, The thermal control of electronic equipment and devices, Adv. Heat Transfer 20 (1990) 181–314.
[5] M. Afrid, A. Zebib, Natural convection air cooling of heated components mounted on a vertical wall, Numer. Heat Transfer A 15 (1989) 243–259.
[6] H.Y. Wang, F. Penot, J.B. Sauliner, Numerical study of a buoyancy-induced flow along a vertical plate with discretely heated integrated circuit packages, Internat. J. Heat Mass Transfer 40 (1997) 1509–1520.
[7] T.J. Heindel, S. Ramadhyani, F.P. Incropera, Conjugate natural convection from an array of discrete heat sources: Part 1. Two- and three-dimensional model validation, Internat. J. Heat Fluid Flow 16 (1995) 501–510.
[8] A. Khalilollahi, B. Sammakia, Unsteady natural convection generated by a heated surface within an enclosure, Numer. Heat Transfer A 9 (1986) 715–730.
[9] Y.L. Tsay, Transient conjugated mixed-convective heat transfer in a vertical plate channel with one wall heated discretely, Heat Mass Transfer 35 (1999) 391–400.
[10] D. Wroblewski, Y. Joshi, Transient natural convection from a leadless chip carrier in a liquid filled enclosure: a numerical study, J. Electronic Packaging 114 (1992) 271–279.
[11] S.V. Patankar, Numerical Heat Transfer and Fluid Flow, Hemisphere, McGraw-Hill, Washington, DC, 1980.
[12] T. Hayase, J.A.C. Humphery, R. Grief, A consistently formulated QUICK scheme for fast and stable convergence using finite-volume iterative calculation procedures, J. Comput. Phys. 98 (1992) 108–118.